



Strength Capacity Cracks Propagations Deflection and Tensile Enhancement of Reinforced Concrete Beams Warped by Glass Fiber Reinforced Polymer Strips

M. M. Abbass^a, M. K. Medhloom^b, I. F. Ali^c

^a Consultant Structural Engineering Baghdad, Iraq

^b Department of Civil Engineering College of Engineering Al Mustansiriyah University, Baghdad, Iraq

^c Ministry of Transport and Communications, Baghdad, Iraq

PAPER INFO

Paper history:

Received 05 October 2020

Received in revised form 12 December 2020

Accepted 29 December 2020

Keywords: Cracks

Propagations Composite

Action Tensile Strength

Glass Fiber Reinforced Polymer

Strength Capacity

ANSYS

Finite Elements

ABSTRACT

Different approaches were adapted to strength the structural elements to increase the load capacity and reduce the deformation such as deflection. The easiest and light external strengthening of reinforced concrete members are Fiber Reinforced Polymer (FRP) family such as Aramid, Carbon, Glass and Basalt, respectively. This paper presents the theoretical approach to check out the experimental tests of reinforced concrete beams strengthened by glass fiber reinforced polymer (GFRP) using finite elements method by ANSYS software in which all models are simulate the tested beams. All models have the same geometry and mechanical properties but differ in GFRP layers and width. The main objectives of present work are evaluating the strength capacity, cracks propagations, deflection and tensile enhancement of reinforced concrete beams warped by GFRP strips subject to four points static load. Analysis of results indicate that the presences of GFRP sheets enhance the capacity and ductility of reinforced concrete beams in additional to delay the post crack concrete. The delay in the formation of first crack, increase in the number of cracks and ultimate loads of the models compared with the control model. There are improvements in flexural strength based on the modulus of rupture. Also, the cracks propagation become less in case of presence of GFRP and there is improvements in tensile resistance due to flexural. Analysis results indicated that the presence of GFRP at the bottom face of reinforced concrete beam in case of two layers gave increase in ultimate load 104.3% as compared with the control model. The reduction of the deflection for same models is 10.84%. Factor of the modulus of rupture range between (0.76-1.36) that is more than with ACI code suggested as 0.6. All model results were close to the experimental tests.

doi: 10.5829/ije.2021.34.05b.03

NOMENCLATURE

Symbol

A_f	GFRP area (mm ²)	M_n	nominal flexural strength (N-mm)
c	Distance from extreme compression fiber to the neutral axis (mm)	M_u	factored moment at a section (N-mm)
d	distance from extreme compression fiber to centroid of tension reinforcement (mm)	β_1	ratio of depth of equivalent rectangular stress block to depth of the neutral axis
f_{fu}	design ultimate tensile strength of GFRP (MPa)	ϕ	strength reduction factor
f_s	stress in steel reinforcement (MPa)	Ψ_f	GFRP strength reduction factor = 0.85 for flexure (calibrated based on design material properties)
h	overall thickness or height of a member (mm)	M_n	nominal flexural strength (N-mm)

1. INTRODUCTION

Concrete as a material is very weak to resist tensile stress that developed in tension concrete zone due to

applied loads. When the internal stress in the structural members increased the cracks will increase [1]. The mechanical properties of GFRP high strength to weight ratio, lightweight and giving better solution for strengthening. Hence, adopt in structural members. Strengthening reinforced concrete beam by GFRP with orientation of fiber reinforcements along the beam

*Corresponding Author Email: mohammadmakki2003@gmail.com (M. M. Abbass)

increasing flexural resistance of beam, stiffness, reduce in deflection and enhance the tensile strength so that the cracks reduced [1]. Wrapped of a simple reinforced concrete beams by FRP layered showed the beams were carried excessive uniform loads in flexure when the layers in the bottom face [2]. The models of simply supported concrete beams that simulated by finite elements approach gave the same behavior and failure modes the same as the reinforced concrete beams strengthened by FRP laminates but differed in capacity, deflection and stress. Applied FRP strips for concrete members increased in the strength to improve the reinforced concrete beams [3, 4]. Presence of GFRP in bottom of reinforced concrete beam showed high post crack and enhanced the strength capacity of reinforced concrete beams [5]. The relative displacements that developed in concrete surface and GFRP was proportional [6]. GFRP recover damage of reinforced concrete members with excellent durability against environment [7]. Presences of FRP lead to increase the shear strength capacity of the reinforced concrete continuous beam over than 25% as compared with the control beam [8]. Modulus of elasticity and yield strength of FRP are affected on the strength capacity of concrete beam and the global average reliability between the unstrengthening and strengthening beams with strips and full wrapped were differ in strength capacity [9]. The rehabilitated and strengthened coupling beams with FRP sheets can achieve appropriate strengths even larger than those of original beams [10]. In case of adopted flexible torsion bar in the design of trailing edge flap system showed a beneficial decreased in torsional stiffness, while increased the bending stiffness of the whole system. In addition, the worm gear drive gave a high torque to overcome aerodynamic force on the flap area and the torsional rigidity of support bar, but also plays as a brake to avoid instability due to the high torsional flexibility of the support bar [11]. The GFRP reinforcement having lower modulus of elasticity, gave in higher deflection than the steel reinforced specimens which have higher modulus of elasticity and the ultimate moment carrying capacity of the GFRP reinforced beam. That beam gave higher than the conventional steel reinforced beam [12]. Automated the printed process lead to make the use of the beam more efficient. This makes the method also attractive for expert users, who want to maximize the quality of their work [13]. The use of FRP composite jackets gave much better performance in terms of ductility as compared with the reinforced concrete reference [14].

2. AIM AND SIGNIFICANT RESEARCH

The aims of present study to evaluate the strength capacity, cracks propagations, deflections and tensile

stress enhancement performance of reinforced concrete beams warped by GFRP located at tension zone and assumed full interactions as surface bound with bottom face of the beams that subjected to four-point static loading using finite elements approach by ANSYS software. The parameters that taking into accounts are GFRP layers and widths. The actual loadings from experimental tests were applied in finite elements ANSYS software to predicate the full performance of reinforced concrete beams strengthened by GFRP and checking with experimental tests.

3. THEORETICAL ANALYSIS

Bonding of GFRP in the tension face of the simply supported reinforced concrete beam to increase the flexural resistance of the reinforced concrete beams, reducing deflection and improve the tensile resistance of concrete against internal tension stress in which the GFRP oriented along the beam span. Therefore, that works as main reinforcement and enhancing the amount of reinforcements in tension zone. Based on ACI – 440 – 2R – 2008 [15], the strength designs of the reinforced concrete beam satisfy Equation (1):

$$\phi M_n \geq M_u \quad (1)$$

The ultimate moment capacity of the reinforced concrete (RC) beam according to ACI – 318 – 2019 [15] was calculated without presences of GFRP (control model). The mode of failure of reinforced concrete beam flexural in case of strengthening with GFRP relay on the crushing of concrete compression zone (when the concrete strain reaching 0.003), plane before the reinforcements yield, or the reinforcements yield and then followed by GFRP sheets tension zone, other case reinforcements in tension zone yield then the concrete in compression level crushing and de-bonding of the GFRP sheets.

The nominal strength as flexural for RC beam strengthening with GFRP calculated by Equation (2) [16]. The ultimate moment with and without presences of GFRP were calculated based on the mechanical properties [1].

$$M_n = A_s f_s \left(d \frac{\beta_c}{2} \right) + \psi_f A_f f_{fe} \left(h \frac{\beta_c}{2} \right) \quad (2)$$

4. MODELS GEOMETRY AND SPECIFICATIONS

Seven models are simulated with the same dimensions and geometry include control model without GFRP while other models differ in GFRP layers and width that matching the real experimental works [1]. The model

dimensions that simulates by ANSYS (150x150x700 mm) in which the span beams are 620 mm with total reinforcements are located at the bottom ($2\phi 8$) and ($2\phi 4$) at top, the stirrups $\phi 6@90$ mm c/c as shown in Figure 1. The total length of GFRP layer is 580 mm along the beam span [1], Tables 1 and 2 lists the models details and material mechanical properties. The model mark is COMPW-N in which COMP is composite model, W is the GFRP width, N is number of layer. Stress-strain behavior reinforcement assumed that elastic-full plastic is shown in Figure 2. Figure 3 stress-strain curve for concrete and Figure 4 is devoted to GFRP. The GFRP thickness is 0.43 mm.

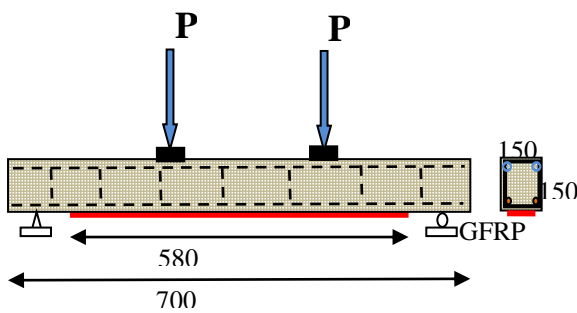


Figure 1. Model dimensions (all in mm)

TABLE 1. Beams model specification

Model mark	CO MP 25-1	CO MP 25-2	CO MP 50-1	CO MP 50-2	CO MP 100-1	CO MP 100-2	RC w/o GFRP P
GFRP width (mm)	25	25	50	50	100	100	NA
Number of layer	1	2	1	2	1	2	NA

TABLE 2. Material mechanical properties

Concrete		Reinforcements		GFRP	
f_c (MPa)	E_c (MPa)	f_y (MPa)	E_s (MPa)	f_y (MPa)	E_s (MPa)
40	36450	420	200000	875	75900

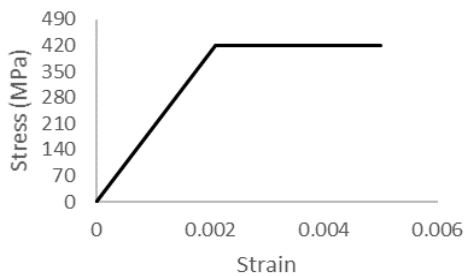


Figure 2. Stress-strain for reinforcement

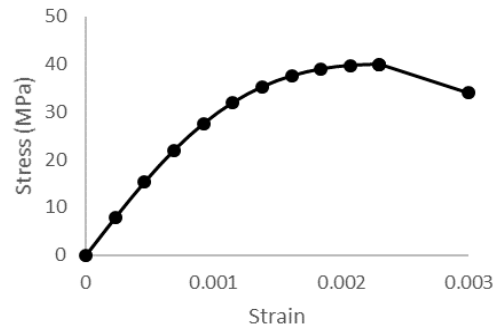


Figure 3. Stress-strain for concrete

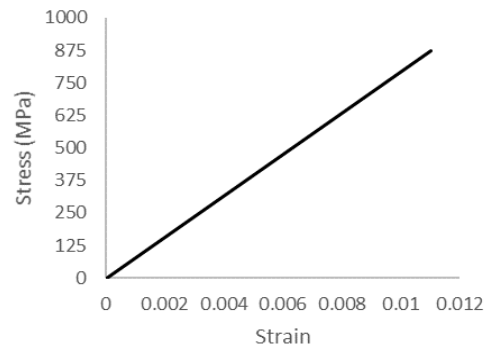


Figure 4. Stress - strain for GFRP

5. NUMERICAL APPROACH

Average load capacities were taken from the previous test [1] that adopted and applied to the models that is simulated by ANSYS [17]. The loads were applied under four points and the models were run as static analysis. The model is divided into a numbers of small elements, 70 elements longitudinal direction (each element is 10 mm), 12 elements in width and depth directions that mean each element is 12.5 mm. All lines within the beam model are divided to produce meshes, lines meshes adopted after many trails to select the mesh size to get near close solutions. The connections between rebar nodes is similar to the concrete solid nodes, so that the concrete and steel reinforcement nodes are merged (full interaction, no slip and friction). The same approach was adopted for GFRP composites. The tolerance value of 0.05 is used as displacement control during the nonlinear solution for convergence.

6. FINITE ELEMENTS MODELING

Numerical analysis using finite elements approach by ANSYS software is adopted to simulate all reinforced concrete beams strengthened by GFRP including the control model. Different elements were selected to

represent the actual behavior of concrete, plate supports, plate under loads, reinforcements as main and stirrups and GFRP layer. SOLID65 element used for concrete material in which three degrees of freedom at each nodes plus translations. LINK180 element is adopted to simulate all steel reinforcement. SOLID185 is chosen to represent the steel plates that locates under the applied loads and supports. SHELL181 element is used to simulate GFRP layer due to this element having membrane (in-plane) stiffness [17]. Smeared crack is the best representation of reinforced concrete members such as adapt beam. The open and close coefficients for concrete cracks were 0.2 and 0.7 respectively. The materials nonlinearity for steel rebar's and concrete are behaved as elastic – full plastic reinforcements, concrete linear up to $0.3fc'$, elastic up to $0.85 fc'$, maximum value of concrete strain is 0.003. The main assumptions of numerical analysis for the plane section remain plane before and after applied loads, the concrete is homogeneous, full bounds between concrete and reinforcements, full interactions between the concrete and GFRP layers and the material nonlinearity of GFRP is linear up to failure and the self-weight of beam not considered in analysis that match the experimental tests. Figure 5 shows the beam model meshes. Figure 6 shows the main and stirrupd reinforcements, Figure 7 shows the wireframe model. In addition, Figures 8, 9 and 10 shows the GFRP elements of model COMP25, COMP50 and COMP100, respectively.

7. LOADING AND SUPPORTS CONDITIONS

The average of three applied load for each specimen that tested for each beam are lists in Table 3. All applied loads adopted from tested beams [1].

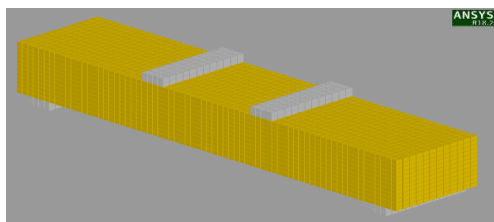


Figure 5. Beam model meshes

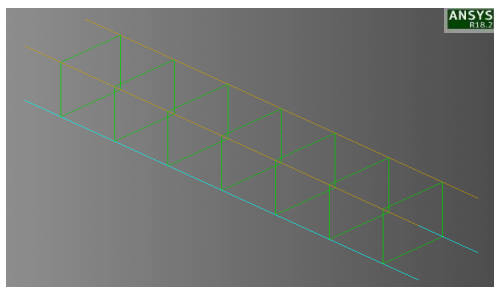


Figure 6. Main and stirrups reinforcements elements

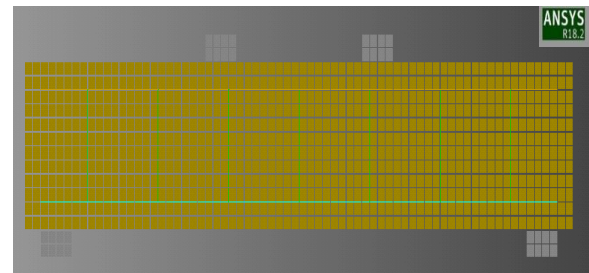


Figure 7. Model wireframe

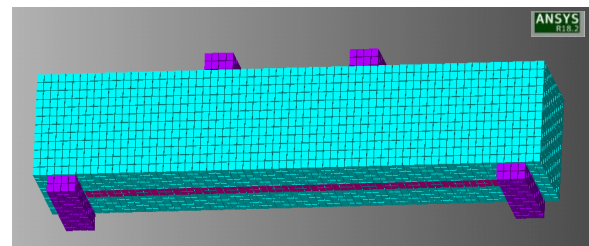


Figure 8. Model COMP25

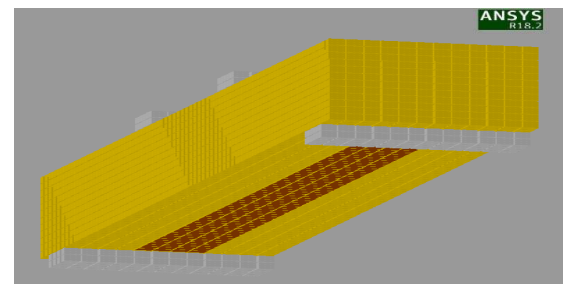


Figure 9. Model COMP50

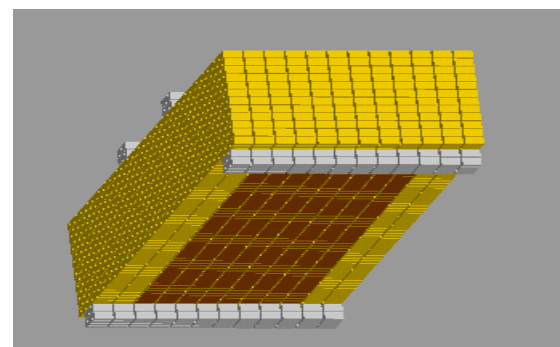


Figure 10. Model COMP100

The loads are divided into series of point loads that applied at the top center line of the upper plates. The supports conditions are simply supported in which the left support simulated as roller that zero displacement in vertical direction. The right support is pin so that restraint in longitudinal and vertical directions. The loads were applied at the central upper nodes that located at the tops of steel plates in which the loads

TABLE 3. Applied loading (average)

Speciman mark	Specimen No.	Load (P) from tests (kN) [1]	Average loading (kN) 2P
COMP25-1	1	31	68
	2	*20	
	3	37.5	
COMP25-2	1	38	72
	2	34	
	3	32	
COMP50-1	1	33	70
	2	38	
	1	48	
COMP50-2	2	49	98.5
	3	51	
	1	46	
COMP100-1	2	53	95
	3	44.5	
	1	42	
COMP100-2	2	49	91
	1	24	
RC w/o GFRP-control	1	24	48

*Unexpected failure

were distributed through nodes. Figure 11 shows the loads and supports conditions.

8. ANALYSIS RESULTS

The static analysis of all models included the control model such as strength capacity, cracks propagations, deflection and tensile strength caused by flexural loadings, are discussed and compared with the test results [1].

8. 1. Crack Pattern

Figure 12 represents the cracks propagations at the ultimate load stage for all models and compares the cracks intensity with

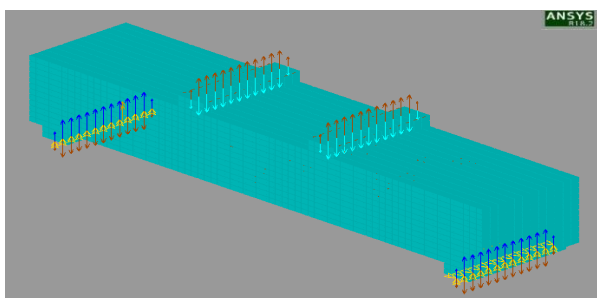


Figure 11. Loads and supports conditions

experimental tests. The circular shape that lies in the plane represents the cracks while the crushed concrete at the compression zone shown as octahedron. Comparisons of cracks patterns between reference and beam with one layer of GFRP (specimen COMP25-1) at ultimate loadings from experimental test that show same cracks propagations. The cracks concentration become less in presence of GFRP at the same loading of reference that means the GFRP makes the reinforced concrete beam more ductile and there is improvement in elastic deformation of the reinforced concrete beams at early stage of applied loads. The modulus of rupture and splitting tensile strength f_{cr} and f_{ct} are based on ACI-318 – 2019, respectively [16] stated as follows:

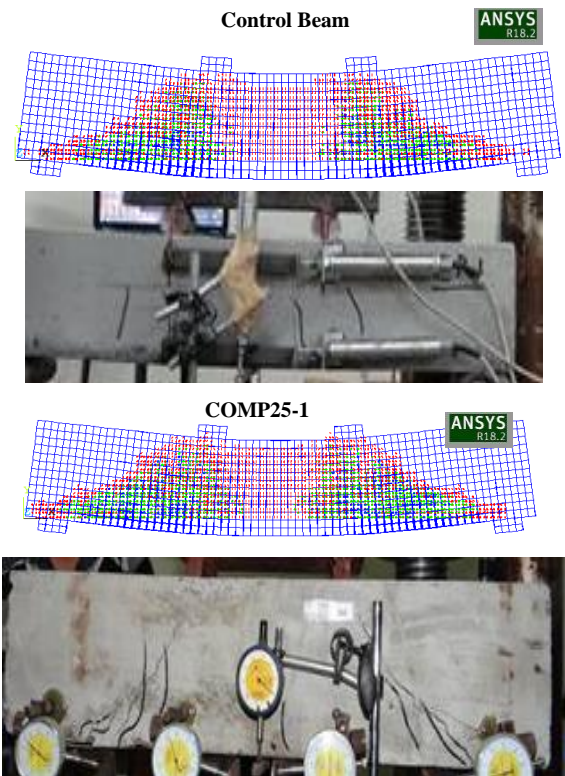
$$f_{cr} = 0.56(f_c')^{0.5} \tag{3}$$

$$f_{ct} = 0.60(f_c')^{0.5} \tag{4}$$

Based on the numerical analysis the load caused first crack lists in Table 4. The factor (k) 0.56 and 0.6 if increased that means there is improvement in tensile resistance of concrete in tension zone due to tensile load and bending, respectively. Also, there is improvement in elastic deformation for each specimen. The new values of the factor in presence of GFRP based on the crack loadings from numerical analysis lists in Table 4 with the new values of factor (k).

8. 2. Load-Deflection Behavior

Figures 13 to 18 represent the deflection behavior of all models at



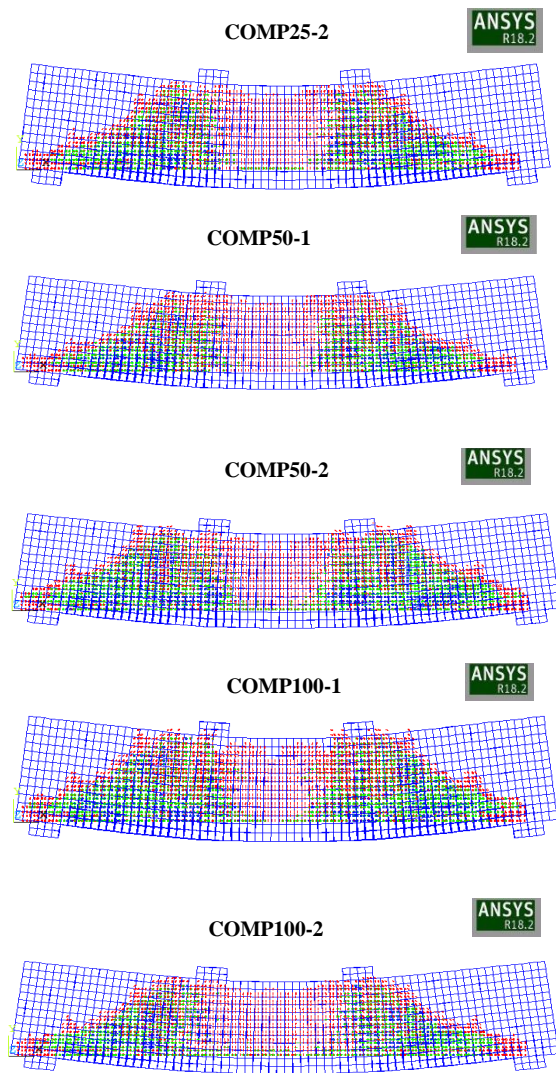


Figure 12. Cracking of the control and RC beams strengthening by GFRP Strips

TABLE 4. First crack loadings, modulus of ruptures and the factor *k*

Model mark	COMP 25-1	COM P 25- 2	COM P 50- 1	COM P 50- 2	COM P 100-1	COM P 100-2
Crack loading (kN)	26	36	34	46	44	47
Modulus of rupture (MPa)	4.77	6.62	6.25	8.45	8.09	8.63
Factor <i>k</i>	0.76	1.05	0.99	1.33	1.28	1.36
%Enhancements of factor <i>k</i>	26.6	75.0	65.0	121	113.	126

ultimate applied load, all model results show close with that in test results. Figure 19 shows the full performance of load-deflection for all models that compare with experimental behavior. The difference between the changes in slopes at various ultimate load levels of the seven beams is a direct result of composite and non-composite behavior. When the load is applied gradually, at its initial stage, only reinforced concrete section works resisting 15-30% of the applied load. After this point, the composite section kicks in and works in full or partial interaction depending on the type of connection between RC beam and GFRP. RF represents reference beam, up 50% of maximum applied loading is linear and within elastic range and serviceability. After that around 76% become nonlinear that means in the range of elastic – plastic and first cracks developed due to increase in loading and the slop become along the longitudinal direction indicated that the material become weak. The next performance is full nonlinear and the slop become toward horizontal up to failure. COMP25-1 up to 25% of maximum applied loading is linear and within elastic range and serviceability, after that around 80% become nonlinear that means in the range of elastic – plastic and first cracks developed due to increase in loading. The behavior of composite is better than that reference beam because of in presence of GFRP delay the cracks in tension face because it is enhancement in resistance tensile strength of concrete tension zone become more resistance. After cracks developed a full nonlinear and the slop become toward horizontal up to failure due to decrease in the beam stiffness because that increase in loads that lead increase the deflections. All other beams, linear up to 22% of maximum applied loading and cracks developed around 86% because of the same reasons mentioned above. COMP25-1 to COMP100-2 are linear and after that become nonlinear according to capacity of composite beam that is really on the number of GFRP layers and scheme layout. The behavior of composite beam rely on where, width and number of layers to re-strengthening RC beam. The permissible deflection values for structural members are listed in the ACI 318-2019 code [16]. According to this reference, the maximum allowable deflection for simply supported beams under service loads should not be greater than $L/360$. Therefore, the maximum deflection of a beam 680 mm span becomes equal to 1.723 mm. However; if FRP is used, then the deflection ratio changes and according to ACI 440-2R [15], the maximum deflection ratio for composite beams (beams with GFRP) is $L/250$, which results become approximately 2.48 mm-deflection. Table 5 lists the comparisons between the experimental and finite elements approach as maximum deflections and compare the models results with control model. Mean value founded from statistical analysis and the standard deviation, variance and coefficient of correlation as the

ratio for numerical results and experimental tests showed closed. Figure 20 shows the performance of load and deflection results with number of layers of GFRP. Increase GFRP layer width that lead to increase the value of load beam capacity and reduce deflection due to increase in beam stiffness, reinforcement in tension zone and make the concrete more ductile due to presence of GFRP sheet. Deflections and crack intensity of models with GFRP strips have higher elastic modulus and moment of inertia due to composite action of reinforced concrete neams wrapped by GFRP strips are less than at the same load contrl model. Analysis results of the numerical simulations clearly showed that beam capacity, stiffness degradation and failure mode of failure are significantly influenced by the GFRP widths and thickness. GFRP makes the concrete more ductile so that reducing in deflection and cracks become less. The reduced in deflections and cracks due to composite beam delay the formation of plastic hinge that make the deflection at first crack load to the maximum deflection less si that the ductility increase in presence of GFRP sheets.

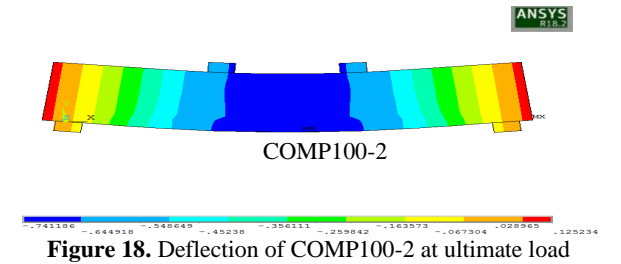
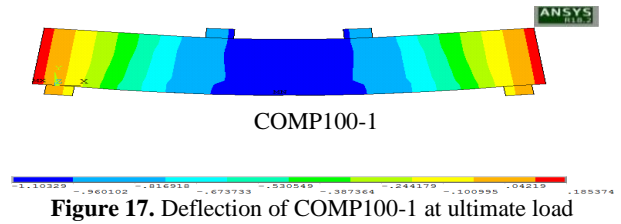
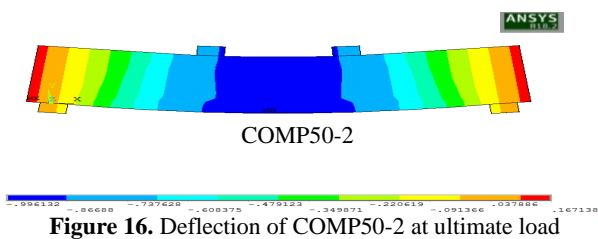
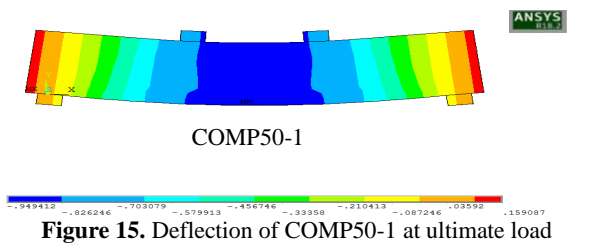
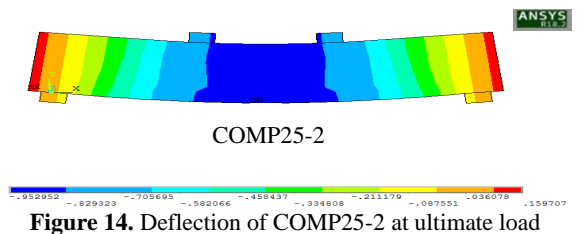
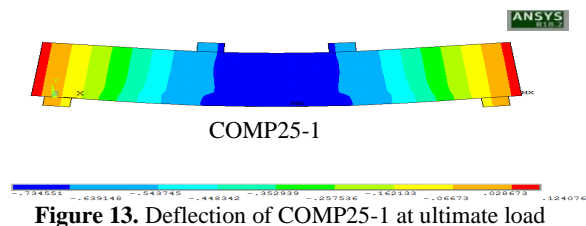


TABLE 5. Comparison results

Specimen mark	Specimen No.	Max.Deflecti on Tests (mm) [1]	Max.Deflecti on FEM (mm)	Ratio (Max. deflection-test/Max. deflection FEM)	Deflection at loading from reference beam (mm) - FEM ANSYS
COMP25-1	1	0.78	0.73	0.94	0.73
	2				
	3				
COMP25-2	1	0.94	0.95	1.01	0.71
	2				
	3				
COMP50-1	1	0.78	0.95	1.01	0.69
	2				
	3				
COMP50-2	1	0.98	0.99	1.01	0.61
	2				
	3				
COMP100-1	1	1.18	1.10	0.93	0.65
	2				
	3				
COMP100-2	1	0.75	0.74	0.99	0.49
	2				
RC w/o GFRP- RF	1	0.88	0.83	0.94	0.83
Mean					0.98
Standard deviation					0.037
Variance					0.0014
Coefficient of correlation					0.85

8. 3. Principle Stresses and Principle Straines

The plane that make angle with the beam axis have a point that lie in this plane occur maximum normal and shearing stresses. Such plane is the principle plane that is developed principle stresses. Increases in applied load make increase in internal tension stress at the location of tension zone that creating cracks so that principle stresses with direction 45° that lead to diagonal cracking as shown in Figure 12 which is perpendicular to the planes of principle tensile strength. To prevent dangerous or decreasing the cracks within limit, GFRP strips used to enhance the tensile behavior of reinforced

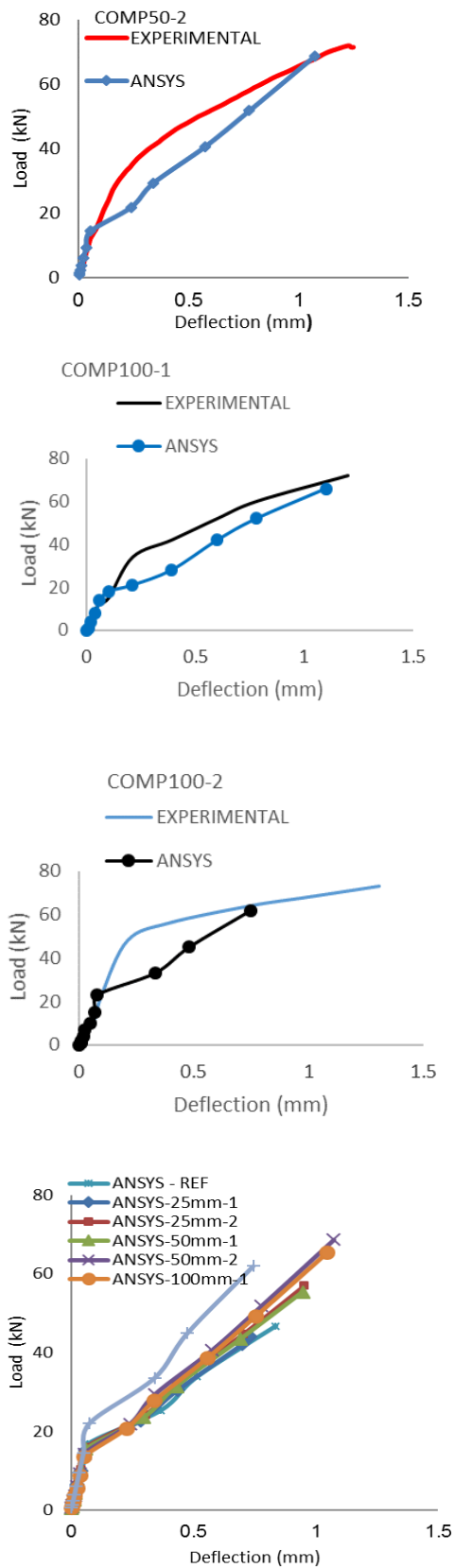


Figure 19. Load–deflection curves for all modeling that compared with test results

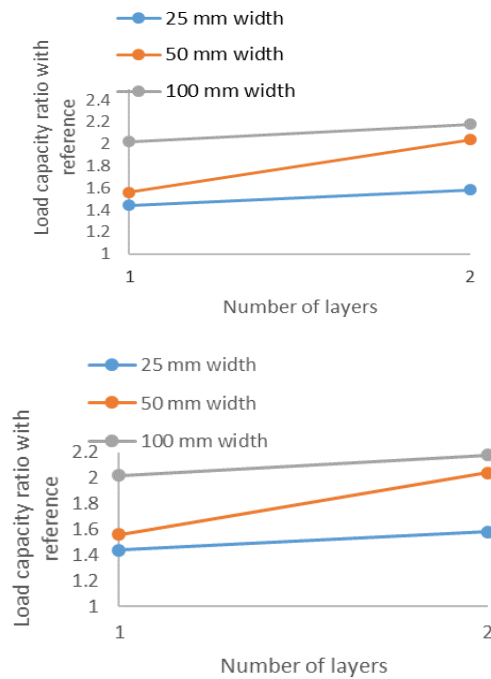


Figure 20. Behavior of load-deflection results with number of layers of GFRP

concrete beam. Figure 21 shows the principle stress for reference beam that the stresses concentrated and directed vectors toward the top. Figure 22 represents the principle stresses of beam strengthened by GFRP 2 layers, so the principle stresses vector toward the bottom and there are a concentration of stresses there. The principle strain for reference beam and strengthening beams presented in Figures 23 and 24, respectively. The principle strain at ultimate load it is more concentrated than in case of reference beam, so that presence of GFRP make the RC beam more ductile and the strain reduced, the deflection and tensile stresses reduced. The Von Mises criteria (yield criteria) which is written as follows:

$$(\sigma_1 - \sigma_2)^2 + (\sigma_1 - \sigma_3)^2 + (\sigma_2 - \sigma_3)^2 = 2f_y^2 \tag{5}$$

In which σ_1 , σ_2 and σ_3 represent first, second and third principle stress and f_y is the yield strength. The vector principle stresses represent the stress path through the model due to applied load. Principle stress shown in Figure 21 different distributions, Figure 22 for beam with GFRP100-2 due to presences of GFRP that concentrated vectors at the bottom at the location of GFRP that sustained and increase the strength capacity of the beam and increase in flexural resistance due to increase in whole beam stiffness. Based on the numerical analysis of the models, the failure criteria that adopted are flexural not shear or torsion. Failure occur

for all models in concrete without spalling of GFRP due to reach the concrete ultimate experimental loads that applied from experimental tests [1]. The vector stress distributions of beam with GFRP100-2 more intensity than control beam model under the neutral axis in the zone of tension zone near tensile reinforcing and GFRP that assumed cracked that means there is concrete tension enhancement in this zobe.

9. STRENGTH CAPACITY OF REINFORCED CONCRETE BEAM BASED ON ACI-318 AND ACI-440-2R

Figure 25 shows the point's distributions around the 45° line that represent the experimental test results and the analytical analysis results for strength capacity of reinforced concrete beam with and without GFRP strips.

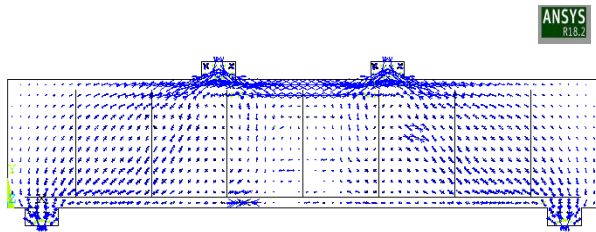


Figure 21. Principle stress vector of control beam

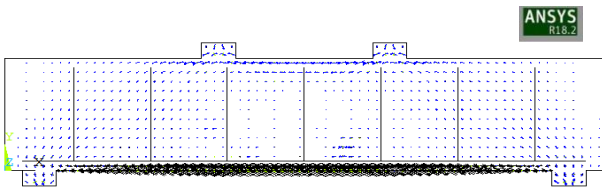


Figure 22. Principle stress vector of beam with GFRP100-2

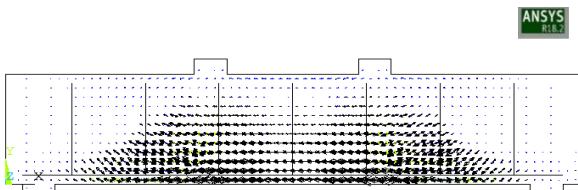


Figure 23. Principle strain vector of beam control beam

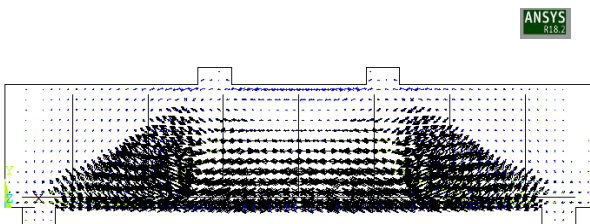


Figure 24. Principle strain vector of with GFRP100-2

Figure 26 represents the deflections at failure load. The point's lies about and close to the straight line that indicates the numerical analysis results are conservative. Table 6 lists the maximum load capacity based on ACI-318 and ACI-440-2R that compare with the experimental test results.

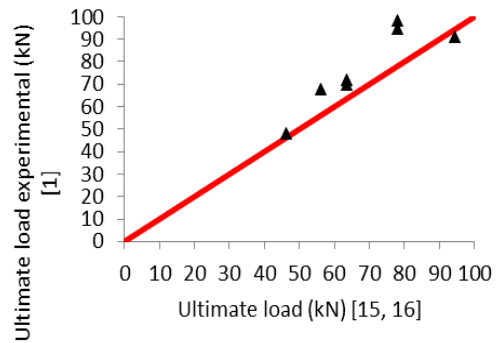


Figure 25. Comparisons between experimental and analytical analysis ultimate load capacity

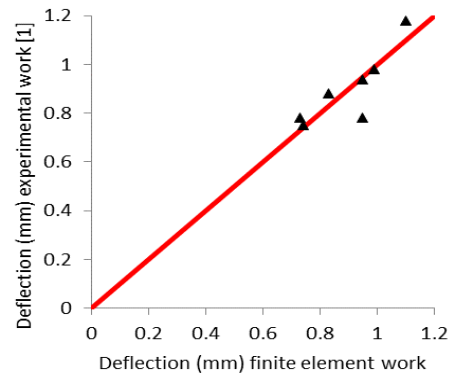


Figure 26. Comparisons between experimental and numerical analysis deflection at ultimate load

TABLE 6. Comparisons between average experimental and theoretical ultimate loads

Spaceman mark	Average loading (kN) 2P-Exp.	Loading (kN) 2P-ACI-440-2R [15]	% (Exp./Theoretical)
COMP25-1	68	56.25	120.88
COMP25-2	72	63.65	113.11
COMP50-1	70	63.65	109.97
COMP50-2	98.5	78.15	126.04
COMP100-1	95	78.15	121.56
COMP100-2	91	94.5	96.35
RC w/o GFRP-control	48	46.25 [16]	103.78

10. DISCUSSIONS AND CONCLUSION

In this paper, numerical analysis using finite elements approach by ANSYS software and analytical solution results using formula presented in ACI-440-2R-08 [15], several conclusions may be drawn as follows:

1. Analysis results of the numerical simulations clearly showed that beam capacity, cracks intensity, deflections tensile resistance and mode of failure are significantly influenced by the GFRP layers and widths. Results from analytical solution for ultimate load capacities showed close with that in experimental tests. Flexural strengthening of reinforced concrete beams with the GFRP sheets is effective, as significantly improved the flexural performance in which in case of two layers of GFRP gave ultimate load 94.5 kN; while, the control model gave 46.25 kN that was increased by 104.32%, the reduction of the deflection for same models as COMP100-2 with RC w/o GFRP-control the reduction is 10.84%. The delay in the formation of first crack and the increase in the number of cracks and ultimate loads of the models compared with the control model. Increasing the layer width and amount of the strengthening layers improved the flexural performance of the models compared with the control model. The model COMP100-2 compared with the model COMP50-2, an increase in ultimate strength is 20.92%.
2. Presences of GFRP layers minimized the cracks proportions due to there is enhancement in tensile resistance for reinforced concrete beam. The presence structure material like GFRP in the tension zone increase the concrete resistance against bending that lead to increase in the tension stress that developed inside concrete in the tension zone. The crack patterns at the final loads from the finite element models correspond well with the observed failure modes of the experimental beams.
3. Two layers of GFRP improve the serviceability, flexural performance and increase strength beam capacity. model COMP100-2 compare with the model COMP100-1, an increase in ultimate strength is 20.92%.
4. Increase in GFRP width become more effective to enhancement the beam performance such as reduce in deflection, increase load capacity and reduce in cracks intensity. COMP100-2 compare with the model COMP50-2, the decrease in deflection is 25.25%.
5. All strengthening beams modelling including control beam "reference beam" as compared with tests result as deflection in case of values and general behaviour listed in Table (5) showed a closed result, so the verification levels results had shown a good agreement between FE modelling procedures using ANSYS and the results from tested results published before [1]. The mean value is 0.98 that is close to unity.
6. Presence of GFRP in tension zone delay in load that cause first crack that lead to delaying earlier failure and shifting failure load to increase. The presences of GFRP plies are useful to enhance concrete member behaviour in resisting loads. In case of two layers of GFRP model COMP100-2 gave crack load 47 kN while the control model gave 25 kN that lead to 88% zone delay in load that cause first crack. Presence of GFRP delays the post cracking of reinforced concrete beam. The concrete cracks in model analysis due to the principal stress are tensile with a crack plane normal to this principal stress. Based on the first crack loadings in case of presence of GFRP that make the factor k become more that indicates there is improvement and enhancement in the tensile stress in tension zone due to flexural loadings. The increase in factor k in case of increase in width COMP100-2 with COMP50-2 and layers model COMP100-2 compare with COMP100-1 were 2.26% and 6.25%, respectively. Increase in factor k that indicate there is enhancement in elastic deformation that lead the first crack loadings become more in case of increase GFRP layer or increase in width of GFRP. Increase in factor k that make the concrete strain increase that indicate the concrete become more ductile.
7. Analysis results from finite element models has some difference as compare with test results due to in model in finite elements slightly more stiffness than the actual experimental tests and the effects of bond slips and the developed micro-cracks occurred in the actual beams were excluded in the finite element models.

11. REFERENCES

1. Abbass, M.M., "Enhancement of the tensile strength of reinforced concrete beams using gfrp", *International Journal of Scientific Engineering and Technology*, Vol. 3, No. 12, (2014), 1424-1430. doi.
2. Ali, F.F., Shawky, R.M. And Al-Sayed, A.-T.A., "Finite element modeling of strengthened simple beams using frp techniques," a parametric study", Vol. 2, No. 2, (2011).
3. Viradiya, S.R. and Vora, T.P., "Comparative study of experimental and analytical results of frp strengthened beams in flexure", *International Journal of Research in Engineering and Technology*, Vol. 3, No. 4, (2014), 555-561. doi: 10.15623/ijret.2014.0304097
4. Tarigan, J., Patra, F.M. and Sitorus, T., "Flexural strength using steel plate, carbon fiber reinforced polymer (CFRP) and glass fiber reinforced polymer (GFRP) on reinforced concrete beam in building technology", in IOP Conference Series: Earth and

- Environmental Science, IOP Publishing. Vol. 126, No. 1, 012025.
- Goldston, M., Remennikov, A. and Sheikh, M.N., "Experimental investigation of the behaviour of concrete beams reinforced with gfrp bars under static and impact loading", *Engineering Structures*, Vol. 113, (2016), 220-232. doi: 10.1016/j.engstruct.2016.01.044.
 - Rashidi, M. and Takhtfirouzeh, H., "An experimental study on shear and flexural strengthening of concrete beams using gfrp composites", arXiv preprint arXiv:1808.10008, (2018). doi: https://doi.org/10.37516/global.j.civ.eng.2019.0047.
 - Siddika, A., Al Mamun, M.A., Alyousef, R. and Amran, Y.M., "Strengthening of reinforced concrete beams by using fiber-reinforced polymer composites: A review", *Journal of Building Engineering*, Vol. 25, (2019), 100798. doi: 10.1016/j.job.2019.100798.
 - Elrawaff, B., Abdul Samad, A.A. and Alferjani, M., "Experimental and theoretical investigation on shear strengthening of rc precracked continuous t-beams using cfrp strips", *International Journal of Engineering*, Vol. 28, No. 5, (2015), 671-676. doi: 10.5829/idosi.ije.2015.28.05b.04.
 - FADAAE, M.J. and Dehghani, H., "Reliability-based torsional design of reinforced concrete beams strengthened with cfrp laminate", *International Journal of Engineering, Transactions A: Basics*, Vol. 26, No. 10, (2013), 1103-1110. doi: 10.5829/idosi.ije.2013.26.10a.01.
 - Mohammadi, H., Esfahani, M. and Riyazi, M., "Behavior of coupling beams strengthened with carbon fiber reinforced polymer sheets", *International Journal of Engineering, Transactions B: Applications*, Vol. 20, No. 1, (2007), 49-58. doi.
 - Ha, K., "Innovative blade trailing edge flap design concept using flexible torsion bar and worm drive", *HighTech and Innovation Journal*, Vol. 1, No. 3, (2020), 101-106. doi.
 - Balamuralikrishnan, R. and Saravanan, J., "Finite element modelling of rc t-beams reinforced internally with gfrp reinforcements", *Civil Engineering Journal*, Vol. 5, No. 3, (2019), 563-575. doi: 10.28991/cej-2019-03091268.
 - Jung, S., Peetz, S. and Koch, M., "Poeam—a method for the part orientation evaluation for additive manufacturing", in Sim-AM 2019: II International Conference on Simulation for Additive Manufacturing, CIMNE., 440-443.
 - Shadmand, M., Hedayatnasab, A. and Kohnehpooshi, O., "Retrofitting of reinforced concrete beams with steel fiber reinforced composite jackets", *International Journal of Engineering, Transactions B: Applications*, Vol. 33, No. 5, (2020), 770-783. doi: 10.5829/ije.2020.33.05b.08.
 - Kuchma, D.A., Wei, S., Sanders, D.H., Belarbi, A. and Novak, L.C., "Development of the one-way shear design provisions of aci 318-19 for reinforced concrete", *ACI Structural Journal*, Vol. 116, No. 4, (2019).
 - Bakis, C.E., Ganjehlou, A., Kachlakev, D.I., Schupack, M., Balaguru, P., Gee, D.J., Karbhari, V.M., Scott, D.W., Ballinger, C.A. and Gentry, T.R., "Guide for the design and construction of externally bonded frp systems for strengthening concrete structures", *Reported by ACI Committee*, Vol. 440, No. 2002, (2002). doi.
 - Ansys manual reference help version 18.2, ansys multiphasic, ansys, inc. Is a ul registered iso 9001:2000 company.

Persian Abstract

چکیده

رویکردهای مختلف برای تقویت عناصر سازه ای برای افزایش ظرفیت بار و کاهش تغییر شکل مانند انحراف، سازگار شدند. ساده ترین و سبکترین تقویت خارجی اجزای بتن آرمه به ترتیب الیاف تقویت شده از خانواده پلیمر مانند مسلح، کربن، شیشه و بازالت (AFRP, CFRP, GFRP و BFRP) است. در این مقاله رویکرد نظری برای آزمایشی تیرهای بتن آرمه تقویت شده توسط GFRP با استفاده از روش عناصر محدود توسط نرم افزار ANSYS که در آن همه مدل ها تیرهای آزمایش شده را شبیه سازی می کنند، ارائه شده است. همه مدل ها دارای هندسه و خصوصیات مکانیکی یکسانی هستند اما در لایه ها و عرض GFRP متفاوت هستند. اهداف اصلی کار حاضر ارزیابی ظرفیت مقاومت، انتشار ترک، انحراف و افزایش کشش تیرهای بتونی مسلح است که توسط نوارهای GFRP تحت چهار بار استاتیکی تاب خورده است. نتایج تجزیه و تحلیل نشان می دهد که وجود ورق های GFRP باعث افزایش ظرفیت و شکل پذیری تیرهای بتن مسلح می شود تا بتونی بعد از ترک خوردگی به تأخیر بیفتد. تأخیر در تشکیل اولین ترک، افزایش تعداد ترک ها و بارهای نهایی مدل ها در مقایسه با مدل کنترل. بهبودهایی در مقاومت خمشی بر اساس مدول پارگی وجود دارد. همچنین در صورت وجود GFRP میزان انتشار ترکها کمتر می شود و در مقاومت در برابر کشش به دلیل خمش بهبودی حاصل می شود. نتایج تجزیه و تحلیل حاکی از آن است که وجود GFRP در سطح پایین تیرآهن بتن آرمه در صورت وجود دو لایه باعث افزایش بار نهایی ۱۰۴.۳٪ در مقایسه با مدل کنترل می شود و کاهش انحراف برای مدل های مشابه ۱۰.۸۴٪، عامل دامنه مدول پارگی بین (۰.۷۶-۱.۳۶) که بیش از کد ACI به عنوان ۰.۶ پیشنهاد شده است. همه نتایج مدل با آزمایش های آزمایشی نشان می دهد.
